

A physical model of cellular self-organization

Author: Adrià Alonso Salvat

Facultat de Física, Universitat de Barcelona, Diagonal 645, 08028 Barcelona, Spain.

Advisor: Marta Ibañez

Abstract: The formation of spatial patterns is a phenomenon that we can find in nonequilibrium systems. Here we model the dynamics of phytohormone auxin, responsible for plant growth, in a one-dimensional ring of 100 cells. Through the numerical integration of the differential equations that control the dynamics of auxin concentration and through a linear stability analysis of these dynamics, we determine the conditions for the homogeneous stationary state of auxin concentration to be linearly unstable and dynamically evolve to a spatial periodic pattern, in which there are spatial regions with high auxin concentration alternating with spatial zones with low auxin concentration. Finally we establish a comparison with a prototype model of pattern formation, the Swift-Hohenberg model.

I. INTRODUCTION

Both in the animal and plant worlds we find structures that show a spatial organization forming geometric patterns: From the skin of zebras to the disposition of seeds in the sunflower flower, or the fractal geometry of the Roman cauliflower, to name a few. In plants, it has been described that plant growth depends on a hormone which can be found distributed forming periodic structures [1,2]. This hormone is called auxin (indole-3-acetic acid, IAAH) and it participates in a great variety of phenomena inside the plant [1]. Among others, the spatial disposition of the leaves on the stem depends on the heterogeneous distribution of auxin. Also it gives an explanation for the growth or directional change of the plant as a response to external stimuli (tropisms). For example, the inclination of the stem to guide the plant towards the sun is a process mediated by auxin. At present, the scientific community is trying to understand the mechanisms of auxin transport at the cellular level in order to determine how the observed heterogeneous concentrations of auxin arise and to ultimately decipher how the formation of periodic structures in plant tissues emerge [2].

In an aqueous medium, we can find auxin in its neutral (IAAH) or in its ionized (IAA^-) forms [1,3]. Neutral auxin can cross the cellular membrane and travel from cell to cell freely in a diffusive way. We call this transport passive since it does not require any source of external energy. It favours the transport from high to low auxin concentrations, to minimize the free energy [4,5]. On the other hand, auxin in its ionic form can not cross the cellular membrane, since the membrane is formed by a phospholipid bilayer that is mostly impermeable to ions due to the high energy barrier set by electrostatic interactions [4,5]. For this reason, an active mediator of ionic auxin transport across the cell membrane can be important. It has been found the existence of proteins that are responsible for this active transport [1]. In this document we focus our attention on a particular kind: The PIN proteins, which located at the cell membrane

allow the auxin transport out of the cell and can be located in different sides of the cell, thus, establishing a polarization or a privileged direction for the transport of auxin. Many neutral auxin molecules that come into the cell through diffusion, dissociate releasing a proton and being ionized when finding the more basic medium of the cytoplasm. This fact implies that they can not cross again the membrane and become trapped, unless PIN proteins are present, what highlights the important role of these PIN proteins.

H.Jönsson et al. [2] proposed a model which takes into account the two transport mechanisms for each form of auxin, based on previous modelling descriptions (e.g like [3]), and it takes the hypothesis that there is a feed-back between auxin concentration and the distribution of PIN proteins at the different sides of the cells. This feed-back establishes that the PIN proteins are situated at the side of the cell adjacent to cells that have more concentration of auxin. Through this mechanism, a cell with a higher auxin concentration than its neighbours will experience a trend to diffuse auxin to its neighbours (passive transport way) and an influx of auxin (transport mediated by PIN proteins). As the authors described, these elements enable for the emergence of stationary spatially periodic distributions of auxin [2].

II. MODEL AND RESULTS

A. The model for auxin dynamics

The model that we use corresponds to the proposed by *H.Jönsson et al.* [2] and we included production and degradation of auxin [6]. This model simplifies the transport described in the Introduction such that there is no difference between the extracellular medium and the cytoplasm. The basic spatial unit can be considered the cell and its adjacent environment, which are considered as a single spatial point (i , hereafter named the cell). It does not explicitly use the two different forms of auxins. Instead, it assumes the fractions of these two forms to

be constant over time such that the model only considers the action of two transports: The diffusive and the transport mediated by PINs, which has the directionality marked by auxin itself. The model describes the temporal evolution of auxin concentration for a cell through the equation:

$$\frac{dA_i}{dt} = D \sum_{k \in \mathcal{N}_i} (A_k - A_i) + T \sum_{k \in \mathcal{N}_i} (A_k P_{ki} - A_i P_{ik}) + \mu - \frac{\mu}{\mu_0} A_i. \quad (1)$$

A_i represents the auxin concentration of cell i . D is the diffusion coefficient and T is the strength of active transport mediated by PINs. P_{ij} is the fraction of active transport from cell i to cell j . The summation is over the set of neighbours of cell i , represented by \mathcal{N}_i . In our one-dimensional discrete system $k \in \mathcal{N}_i$ takes only two values: The value of the cell on the left, $i - 1$, and the value the cell on the right, $i + 1$. The parameter μ regulates the creation-destruction of auxin, considering a creation constant term that is the same for each cell and a destruction term proportional to the amount of auxin of the cell. μ_0 is the auxin average value, $\mu_0 = \sum_i A_i / N$.

The model in [2] takes a list of hypotheses about the dynamics of PIN molecules. From them, an expression for P_{ij} that only depends on the auxin concentration of neighbours cells can be found [2]:

$$P_{ij} = \frac{A_j}{\sum_{k \in \mathcal{N}_i} A_k}.$$

Therefore, the fraction of active transport from cell i to cell j is proportional to auxin concentration in cell j and inversely proportional to the summation of auxin concentrations of neighbouring cells. That is to say, for our one-dimensional system, if we focus on one cell, the fraction of transport to the cell on the right will be higher as higher the auxin concentration of auxin in this adjacent cell is compared to the concentration of auxin in the cell located at the left. With these considerations, Eq. (1) becomes:

$$\begin{aligned} \frac{dA_i}{dt} = & D(A_{i+1} + A_{i-1} - 2A_i) + TA_i \left(\frac{A_{i+1}}{A_{i+2} + A_i} + \right. \\ & \left. + \frac{A_{i-1}}{A_i + A_{i-2}} - 1 \right) + \mu - \frac{\mu}{\mu_0} A_i \end{aligned}$$

If we divide this equation by T , the equation becomes dimensionless in time, taking as characteristic time-scale $1/T$:

$$\begin{aligned} \frac{dA_i}{d\tau} = & b(A_{i+1} + A_{i-1} - 2A_i) + A_i \left(\frac{A_{i+1}}{A_{i+2} + A_i} + \right. \\ & \left. + \frac{A_{i-1}}{A_i + A_{i-2}} - 1 \right) + m - \frac{m}{m_0} A_i \end{aligned} \quad (2)$$

In this way the equation of our model only depends on two parameters: b and m . b is the efficiency ratio between diffusion and active transport ($b = D/T$) and m

quantifies the amplitude of auxin elimination and creation (for $m = 0$ auxin is conserved and we have a conserved model).

It is easy to verify that the homogeneous state where all cells have the same concentration of auxin is a solution of Eq. (2). To observe the dynamical evolution of auxin concentration in our ring of 100 cells with periodic boundary conditions, we depart from the initial condition where all cells have the same value m_0 (we take $m_0 = 1$, for simplicity on all our calculations) adding a small random perturbation which follows a uniform distribution $[0,1]$ and which has an amplitude of 1% from the homogeneous state $A_i = m_0 = 1, \forall i$. To introduce different initial conditions we used different seeds for the generation of pseudo-random numbers. For the selected

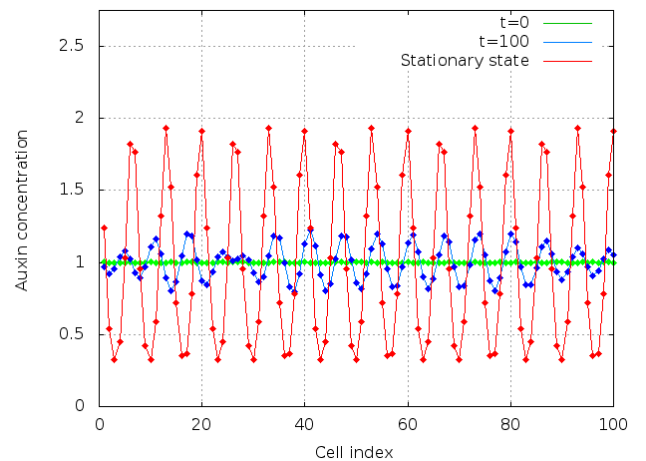


FIG. 1: Resulting pattern for $b = m = 0.1$, at different times.

parameter values ($b = m = 0.1$), the homogeneous solution is unstable and a stationary state with 15 peaks where auxin concentration becomes maximum is formed, as depicted in Fig. (1). Also we observe that the pattern is not symmetric around m_0 since the peaks of maximum auxin have more amplitude than the wells of minimum auxin. This temporal simulation is the result of numerical integration of Eq. (2) with a Runge-Kutta algorithm of first order taking a time step $dt = 0.01$ for 100 cells and periodic boundary conditions.

In the next section we do a linear stability analysis (LSA) [7] to understand how the homogeneous state is unstabilized and the dependence on the model parameters b and m . LSA analysis of this model has been presented in [2] and [6].

B. Linear Stability Analysis (LSA) and its comparison with numerical simulations

We study the stability of the stationary homogeneous state $A_i = A_0 = m_0, \forall i$ by introducing a small perturbation around it: $A_j = A_0 + a_j$, where $a_j \ll A_0$

At first order on a_j , Eq. (2) takes the form

$$\frac{da_j}{d\tau} = \left(-\frac{1}{2} - 2b - m\right)a_j + \left(b + \frac{1}{2}\right)(a_{j-1} + a_{j+1}) - \frac{1}{4}(a_{j-2} + a_{j+2}) \quad (3)$$

where $m_0 = 1$ has been used. Because of the linearisation, these equations describe the dynamics of a small perturbation at early times. The perturbation will either grow or decay. If there is a perturbation that will grow, then the homogeneous state is linearly unstable [7]. Conversely, the homogeneous state will be stable if all perturbations disappear over time, leaving the system on homogeneous state.

We tested with a general solution for a_j of the form

$$a_j = \sum_{k=1}^N \eta_k e^{\frac{2\pi i k j}{N}} \quad [7], \text{ where } i \text{ is the imaginary unit.}$$

The mode k makes reference to a spatial periodicity with k maximums for N cells. The summation is along all possible modes that may be present in a ring of N cells. η_k is the amplitude of the k mode. If we introduce this solution in Eq. (3) we get an equation for the temporal evolution of amplitude of a mode k :

$$\frac{d\eta_k}{d\tau} = \eta_k \mathcal{F} \left(\cos \left(\frac{2\pi k}{N} \right) \right)$$

Where $\mathcal{F}(X) = -X^2 + (1 + 2b)X - (2b + m)$.

Therefore, the homogeneous state will be unstable when there is a k such that $Re(\mathcal{F}(k)) > 0$. At this point, through this LSA, let us see what is the effect of each parameter, b and m , separately (Fig. (2)). Fig. (2) shows

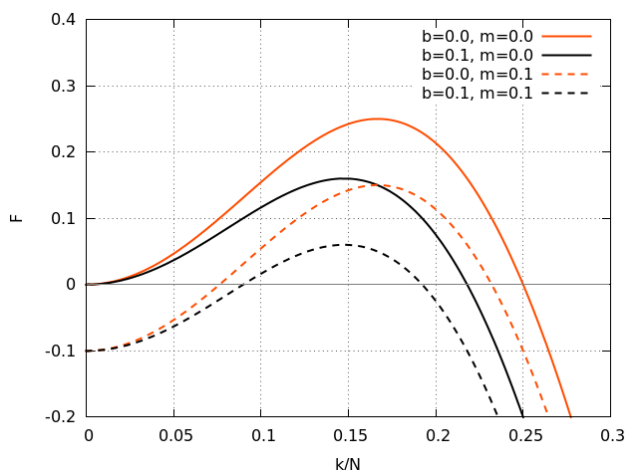


FIG. 2: $\mathcal{F}(\frac{k}{N})$ for different values of b and m . The black dashed curve ($m = b = 0.10$) corresponds to the case shown in Fig. (1).

that varying b changes the k value for which \mathcal{F} is maximum (we defined it as k_{max} and it can be an indicator for the number of peaks that we will expect to find on the resultant pattern). If we calculate this k_{max} analytically

we get the expression

$$k_{max} = \frac{N}{2\pi} \arccos(b + \frac{1}{2}) \quad (4)$$

Fig. (2) also shows that there is a critical b (defined as b_c , for $m = 0$) above which the function \mathcal{F} never takes positive real values and hence any perturbation will decay, the homogeneous state will be stable and a pattern will not be formed. This fact is observed from Eq. (4). We get the conclusion that $b_c = 0.5$ because the function \arccos does not allow arguments higher than 1. Therefore, the strength of active transport will have to be always twice or more the strength of diffusion so that a pattern will be formed. This behaviour of the model with the parameter b confirms what we would expect by an intuitive way: Active transport mediated by PINs favours the apparition of a pattern while the diffusion opposes this.

Later (Fig. (4)) we will speak of a phenomenon that is a consequence of non linear terms and that the LSA can not foresee: peak fusion. This is why we analysed the pattern at small times to observe the dependence between the periodicity and b to compare it with the predictions of the LSA on k_{max} as a function of b . We performed 10 simulations (numerical integration of the dynamics) for each value of b (with $m = 0$), counted the number of peaks that appear at small times for each simulation and took the arithmetic average and standard deviation. On each simulation we started with different initial conditions, namely different seeds on the generation of pseudo-random numbers. The obtained results are shown in Fig. (3) and its comparison with LSA indicates that indeed k_{max} is reporting on the periodicity of the pattern at first order. In Fig. (2) we observe that

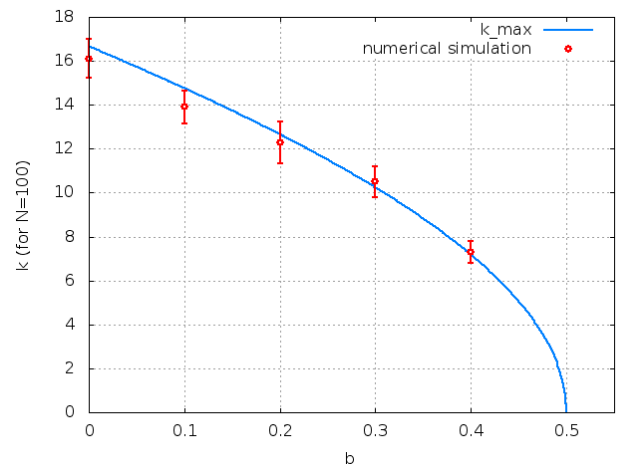


FIG. 3: Theoretical curve $k_{max}(b)$ obtained from LSA and values from the numerical simulation of 10 cases for each value of b , with $m = 0$.

the LSA predicts no dependence between k_{max} and m . In numerical simulations, we confirmed that increasing

the parameter m value does not affect to the number of peaks that we expect find on the resultant pattern, at least for short times. LSA also shows that a $m \neq 0$ makes a finite rank of values for k that unstabilize the homogeneous state, in contrast with increasing b . LSA also indicates that the parameter m has a critical value above which a pattern will not be formed (defined as m_c , for $b = 0$). This value is $m_c = 0.25$ and it coincides with the higher value that the function \mathcal{F} takes for $b = m = 0$.

According the LSA, the effect to increase m is in the characteristic time of growth of the perturbation, as \mathcal{F} plays like the exponential growth ratio of η_k , $\eta_k(t) = \exp(\mathcal{F}t)$ (Fig. (2)). We studied whether this dependence holds in numerical simulations. To carry out this analysis we defined an order parameter z related to the difference with the homogeneous state of auxin concentration:

$$z \equiv \frac{1}{N} \sum_{i=1}^N (A_i - A_0)^2$$

That is to say, z is the squared of the difference between the auxin concentration for each cell and the value of the homogeneous state, added for all cells and divided for the total number of them. The result of numerical simulations is shown in Fig. (4). LSA allows to foresee

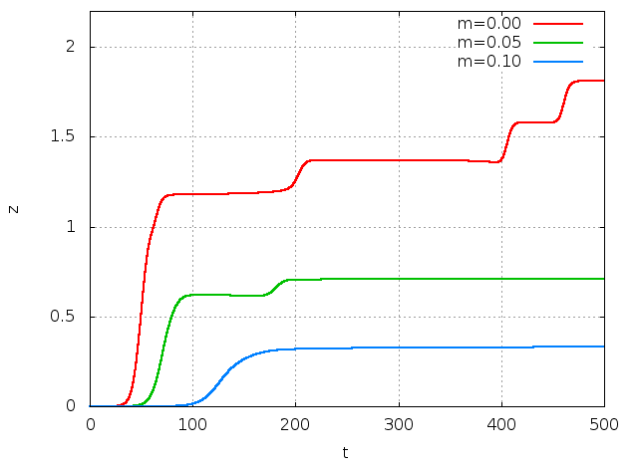


FIG. 4: Temporal evolution of the order parameter z for different values of $m < m_c$, $b = 0.1$. The curve $m = 0.10$ (in blue) corresponds to the case shown in Fig. (1).

when the system will be unstable and it will start the generation of a pattern but it does not get information about when it will become saturated, since this is consequence of non linear terms. In any case, Fig. (4) shows that increasing m implies an increase in the time when the pattern starts to emerge. Increasing m also changes the amplitude of the final pattern because z gives us an idea about how far away the system is in regard to the homogeneous state. If we focus on the curve $m = 0$ we observe a step-like dynamical evolution. This behaviour reflects what we discussed briefly: any time that there is a jump it means that there is a peak fusion. In this

case, for example, the system formed initially 15 peaks, as predicted by LSA, and ended up in 11 peaks on the stationary state. We did few simulations and observed that increasing the parameter m , reduces peak fusion, probably because this restricts the rank of allowed values of k , while increasing b , which is like to say increasing the diffusive transport, favours peak fusion.

Now we establish a comparative between our model and a well-known pattern formation model in nonequilibrium systems in physics, the Swift-Hohenberg model [7].

C. Swift-Hohenberg (SH) model

The one-dimensional SH [7] equation shows the evolution of a single field $u(x, t)$. In a continuous spatial domain it takes the form

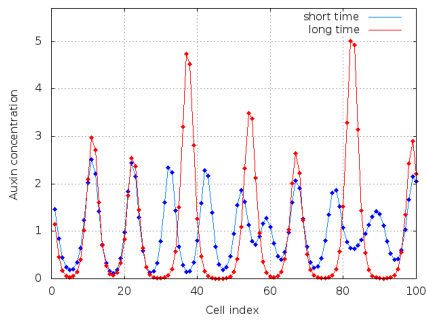
$$\partial_t u(x, t) = ru - (\partial_x^2 + k_0^2)^2 u - u^3 \quad (5)$$

Many phenomena of pattern formation have been investigated by simple changes to the original SH equation [5]. We observe that the SH model has two control parameters, r and k_0 . To bring about the comparative with our model, we take the discrete form of Eq. (5):

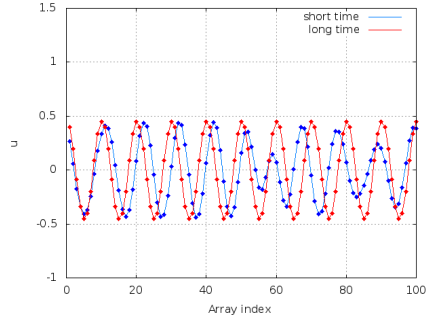
$$\begin{aligned} \frac{du_i}{dt} = & \left(r - k_0^4 + 4k_0^2 - 6 \right) u_i + \left(4 - 2k_0^2 \right) (u_{i-1} + u_{i+1}) \\ & - (u_{i-2} + u_{i+2}) - u_i^3 \end{aligned} \quad (6)$$

If we perform LSA on Eq. (6), just like we did with auxin model, we can observe the analogy with Eq. (3). To match the therms we impose $4 \frac{da_i}{dr} = \frac{du_i}{dt}$. This implies that the characteristic time-scale in SH model will be the fourth part of the characteristic time-scale in auxin model, fact that does not affect us because we will focus on the comparison of two aspects: The periodicity and the possibility that peak fusion could exist in SH model. We take $k_0 = 0.628$ [8] for the SH model and $m = 0$ for the auxin model because we are interested on the case where there is peak fusion. Equalling term to term we get the following values for the other parameters: $b = 0.3$ and $r = 0.1555$.

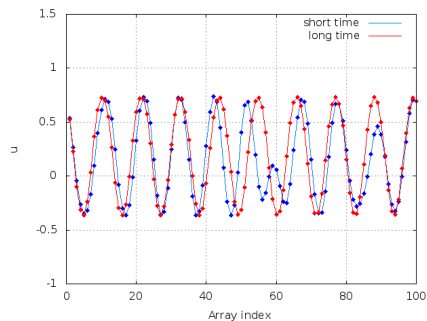
By making numerical integration of the dynamics for the SH model we observe that the periodicity of the pattern is like the periodicity predicted by the LSA and it does not vary along the time, i.e. it is like to say there is no peak fusion. Then we modified Eqs. (5) and (6) adding a squared term with a new control parameter, $+su^2$, and we called this modified SH model. This term does not affect the LSA, and thus the expected periodicity should not vary. The LSA expected number of peaks is 10. We observe in Fig. (5) that at short times the three models (auxin, SH and modified SH) have a total of 10 peaks, but at the stationary state, the auxin model has gone to have 7 peaks, the SH still has 10 peaks, and the modified SH model has gone to have 9 peaks. We



(a) Resulting pattern for auxin model, at different times.



(b) Resulting pattern for SH, at different times.



(c) Resulting pattern for modified SH, at different times.

FIG. 5: Obtained results on the simulations for different models, at short time and on the stationary state.

could think that the effect of the added term on the original SH model is the possibility to have peak fusion but the nature of this is different than the nature in auxin model: In auxin model, when two peaks are fused the result is one peak with an amplitude resulting to the sum of the amplitudes of the two peaks while in the modified SH model the pattern is restructured so that the peaks would have the same amplitude.

III. CONCLUSIONS

- We have numerically integrated a model for the dynamics of auxin hormone transport. We have confirmed that the active directional transport term can unstabilize the homogeneous state, driving a final spatial periodic state, unlike diffusion and the auxin creation-destruction terms, which favour the homogeneous state.
- We have performed LSA and, through comparison with numerical simulations, we have confirmed it is a powerful tool in order to find analytic expressions which inform us about what happens in the model of auxin dynamics, at first order. It predicts the more probable periodicity of the resulting pattern at early times and show analytically it only depends on the parameter b . Also it informs on how long the system takes to become unstable.
- We have compared the auxin model with the SH model. We have established and confirmed the parameter values that set them equivalent at the linear regime. This equivalence is not found in non-linear phenomena like the shape of maximums and the evolution at long times that involves peak fusion. We have shown that introducing a non linear term in the SH model captures partially this phenomenology, supporting that non linearities are involved in these processes.

Acknowledgments

Thanks to my advisor Marta Ibañes for all her help.

-
- [1] B. Alberts, A. Johnson, J. Lewis, M. Raff, K. Roberts, and P. Walter, *Molecular biology of the cell*, (Garland Science, New York 2002, 4th. ed.).
 - [2] Jönsson, H. et al. "An auxin-driven polarized transport model for phyllotaxis". PNAS **103**: 1633-1638 (2006).
 - [3] Goldsmith, M.H. et al. "Mathematical analysis of the chemiosmotic polar diffusion of auxin through plant tissues". PNAS **78**: 976-980 (1981).
 - [4] P. Nelson, *Física Biológica: Energía, información, vida*, (Reverté, Barcelona 2005).
 - [5] R. Phillips, J. Kondev, J. Theriot, and H. Garcia, *Physical Biology of the Cell*, (Garland Science, New York 2012, 2nd. ed.).
 - [6] P. Tondelier, *Pattern formation in growing systems: dynamics of auxin in Arabidopsis*, (Study done for Stage de recherche M2 CFP, Ecole Normale Supérieure - Universitat de Barcelona 2012).
 - [7] M. Cross and H. Greenside, *Pattern Formation and Dynamics in Nonequilibrium Systems*, (Cambridge University Press, New York 2009).
 - [8] J. Garcia-Ojalvo and J.M. Sancho, *Noise in spatially extended systems*, (Springer-Verlag, New York 1999).